

arXiv:2008.00341v2 [astro-ph.GA] 13 Sep 2020

# Mathematical Underpinnings of the Multi-Wavelength Structure of the TRGB

Barry F. Madore<sup>1,2</sup> AND Wendy L. Freedman<sup>2</sup>

<sup>1</sup>*The Observatories*

*Carnegie Institution for Science*

*813 Santa Barbara St., Pasadena, CA 91101*

<sup>2</sup>*Dept. of Astronomy & Astrophysics, University of Chicago*

*560 S. Ellis Ave.,*

*Chicago, IL, 60637*

## ABSTRACT

We consider the application of the tip of the red giant branch (TRGB) in the optical and in the near infrared for the determination of distances to nearby galaxies. We analyse ACS VI (F555W & F814W) data and self-consistently cross-calibrate WFC3-IR JH (F110W & F120W) data using an absolute magnitude calibration of  $M_I = -4.05$  mag as determined in the LMC using detached eclipsing binary star geometric parallaxes. We demonstrate how the optical and near-infrared calibrations of the TRGB method are mathematically self-consistent, and illustrate the mathematical basis and relations amongst these multi-wavelength calibrations. We go on to present a method for determining the reddening, extinction and the true modulus to the host galaxy using multi-wavelength data. The power of the method is that with high-precision data, the reddening can be determined using the TRGB stars themselves, and decreases the systematic (albeit generally small) uncertainty in distance due to reddening for these halo stars.

*Keywords:* distances

## 1. INTRODUCTION

The Carnegie Chicago Hubble Program (CCHP) has been pursuing three goals: (1) Improving the Cepheid distance scale by understanding the optical, and carefully moving to the near infrared (eg., Hoyt et al. 2018; Madore et al. 2018), and (2) Establishing an independent and parallel path to the Hubble constant by building a Population II distance scale, based on RR Lyrae stars, the tip of the red giant branch (TRGB) method (e.g., Freedman et al. 2011; Freedman et al. 2012; Rich et al. 2014; Scowcroft et al. 2016a,b; Beaton et al. 2016; Hatt et al. 2017; Madore et al. 2018, Hatt et al. 2018a,b; Jang et al. 2018; Hoyt et al. 2018; Rich et al. 2018; Beaton et al. 2019; Hoyt et al. 2019), and ultimately (3) An independent calibration of Type Ia supernovae, leading to a determination of  $H_o$  (Freedman et al. 2019, 2020).

The value of the Hubble constant, derived from a cosmological model (e.g., Ade et al. 2016, Planck 2018) has been at variance with classical, locally-determined values. In particular, studies using Cepheid variables at their base (e.g., Freedman et al. 2001; Freedman et al. 2012; Riess et al. 2011;

Riess et al. 2016; Riess et al. 2019) have consistently given values of the Hubble constant around 73–74 km/sec/Mpc, with total quoted errors being on the order of 2 to 3 km/sec/Mpc. These expansion rates are more than 3-sigma larger than the CMB modeling values of  $H_o = 67.4 \pm 0.5$  km/sec/Mpc (Planck Collaboration 2018). Recent results from the H0LiCOW program (Birrer, et al. 2018, Bonvin et al. 2017, Wong et al. 2019) using time delays from strong lensing, interpreted within the context of  $\Lambda$ CDM models, also suggest a value of  $H_o$  around 73 km/s/Mpc with errors currently running in the 2 km/s/Mpc range. A precise and accurate calibration of the absolute magnitude of the TRGB as an independent means of establishing the astrophysical distance scale is of critical importance in resolving the current impasse. Interestingly, the recent TRGB calibration (Freedman et al. 2019) falls between the Planck and other local estimates of the Hubble constant with  $H_o = 69.8 \pm 0.8(stat) \pm 1.7(sys)$  km/s/Mpc.

What has not been well-recognized is that across all wavelengths the colors and absolute magnitudes of the very brightest, first-ascent red giant-branch (RGB) stars are correlated. And this run of tip magnitude with intrinsic color is well understood (and predicted) to be driven by well-defined and monotonic functions of the tip stars’ atmospheric metallicity. Viewed in terms of their bolometric magnitudes, higher-metallicity RGB stars are progressively redder and brighter than low-metallicity stars at the same stage of their evolution (brightening at a rate of about 0.18 mag/dex according to Salaris & Cassisi (1997)). However, the wavelength-dependent, differential line blanketing of the cool (4,000K) stellar atmospheres of these luminous K giant stars, results in *decreasing* luminosities with increasing colors, at wavelengths bluer than about 8000Å. There is a relatively flat response of the tip to color in the I-band, which is followed by an up-turn in the trend with color at near- and mid-infrared wavelengths. In the color-magnitude diagram the slope of the red giant branch (RGB), and then the difference in magnitude between the horizontal branch (HB) and the giant branch (at some fiducial color, e.g., Sandage & Wallerstein 1960; Sandage & Smith 1966; Demarque & Geisler 1963; Hartwick 1968) each have a long history of being used as metallicity indicators of Population II systems. As mentioned above, this metallicity effect decreases in going from the blue to the visual. At red end of the optical range, in the *I* band, the tip of the RGB (TRGB) has been established as one of the most accurate and precise methods for measuring the distances to nearby galaxies (e.g., Lee, Freedman & Madore 1993; Jacobs et al. 2009; Hatt et al. 2017; Jang & Lee 2017; Jang et al. 2018). Beyond that, at near-infrared (*JHK*) wavelengths where the TRGB stars are increasingly more luminous, a new calibration of the TRGB (Madore et al. 2018; Hoyt et al. 2018) shows even greater promise for extending the reach of the TRGB in determining distances on cosmologically significant scales.

In this paper we make explicit the simple mathematical underpinning of the multi-wavelength calibration of the TRGB. This then allows us to understand and apply the TRGB zero point and color-dependence calibration from the optical (*BVI*) and into the near-infrared (*JHK*), and then predict its behavior out into the mid-infrared (beyond 2  $\mu$ m, say). Given that TRGB (spectral type K) stars are intrinsically redder than Cepheids (having F and G spectral types), the absolute magnitudes of TRGB stars rapidly go from being fainter than Cepheids (with periods in excess of 10 days, say) at optical (*BV*) wavelengths, to being competitive in luminosity in the near-infrared at 1.6 and 2.2  $\mu$ m, for example.

We note that fitting the “tip” (interpreted to mean the brightest “point” of the helium-flash-truncated red giant branch) is not a concept that applies at all wavelengths, without some modifi-

cation. At all wavelengths the so-called tip spreads out in color as a function of metallicity, as it simultaneously spreads in luminosity. The TRGB rises in luminosity with increasing color in the redward bands (greater than  $9000\text{\AA}$ , say), falls in the blueward bands, and holds at a fairly constant luminosity (with color/metallicity) at the transitional I-band wavelength. But the changes in luminosity for any given wavelength are deterministically correlated with the corresponding changes in color/metallicity. The near-infrared (K band) luminosity of the modern-day TRGB (as defined by the most luminous RGB stars in globular clusters) was first found, nearly 40 years ago (Frogel, Cohen & Persson 1983), to be a brightening function of color, where they authors rightly attributed this effect to increasing metallicity (their Figures 1, 2 & 4). More recently, with the deployment of panoramic near-infrared detectors, on the ground and in space, several groups have seen this same upward trend of NIR luminosity with increasing color, in extragalactic populations of halo stars having a range of metallicities and colors (e.g., Dalcanton et al. 2012; Wu et al. 2014; Madore et al. 2018; Anand et al. 2019 and McQuinn et al. 2019).

## 2. TRANSFORMATIONS

We begin with one (linear) mathematical realization of the run of the TRGB magnitude with color:

$$M_J = a_1 (J - K)_o + b_1 \quad \dots (1)$$

where  $b_1$  is the  $J$ -band zero point, and  $a_1$  is the slope of the TRGB in the  $J$  band as a function of the intrinsic  $(J - K)_o$  color.

First, it is simple to show that the calibration of the TRGB in the  $K$  band is pre-determined by a simple re-arrangement of terms in Equation 1,

$$M_K = M_J - (J - K)_o = a_1 (J - K)_o + b_1 - (J - K)_o = (a_1 - 1) (J - K)_o + b_1$$

It is worth emphasizing that while the  $J$  and  $K$ -band slopes ( $a_1$  and  $a_1 - 1$ , respectively) differ by unity (exactly unity), their respective zero points are identical (both being equal to  $b_1$ ); this is a mathematical tautology. What is less obvious is that the mapping of the calibration to other wavelengths is equally as simple, and just as deterministic.

For example, let us next seek out a calibration in a different bandpass, the  $H$ -band, say. The key step is to establish how the new color  $(J - H)_o$  quantitatively corresponds to the original  $(J - K)_o$  color. Over the small color range applicable to the TRGB it is reasonable to adopt a linear transformation of the form

$$(J - H)_o = \alpha(J - K)_o + \beta \quad \dots (2)$$

Now, by definition

$$M_H = M_J - (J - H)_o$$

and then combining Equations 1 & 2 gives

$$M_H = a_1(J - K)_o + b_1 - \alpha(J - K)_o - \beta$$

giving

$$M_H = (a_1 - \alpha)(J - K)_o + [b_1 - \beta]$$

Thus, given knowledge of one independently calibrated run of the TRGB magnitude with color, all that is required are the color-color relations between different bandpasses for the small run of spectral types of stars populating the TRGB, in order to predict the slopes and the zero points for all other color-magnitude combinations.

By this same logic we then have the following calibrations for the run of the TRGB as a function of the  $(J - H)_o$  color, where  $(J - K)_o = 1/\alpha(J - H)_o - \beta/\alpha$ , thus

$$M_J = [a_1/\alpha](J - H)_o + [b_1 - a_1\beta/\alpha]$$

$$M_H = [a_1/\alpha - 1](J - H)_o + [b_1 - a_1\beta/\alpha]$$

$$M_K = [(a_1 - 1)/\alpha](J - H)_o + [b_1 - (a_1 - 1)\beta/\alpha]$$

### 3. REDDENINGS SELF-CONSISTENTLY DERIVED BY AND FOR THE TRGB

In one of the earliest applications of the TRGB method to extragalactic distance determinations (e.g., Lee, Freedman & Madore 1993) it was (plausibly) argued that reddening corrections would be small (and/or, could be reasonably well-estimated independently) for any given line of sight. This follows from the following two lines of argument: (1) In any given galaxy the old Population II stars (of which TRGB stars are amongst the brightest components) make up the bulk of mass and light in the halo. Halos are generally gas- and dust-free. Thus by limiting observations to the halos of galaxies, any reddening corrections are significantly decreased as compared to the disk, for example, where Cepheids are located. (2) Maps of the Milky Way foreground extinction (Schlafly & Finkbeiner 2011, Schlafly, Finkbeiner & Davis 1998; Burstein & Heiles 1982) can then be used to estimate the only other (independent) source of extinction affecting the observed TRGB magnitudes.

Under extreme conditions, where the target galaxies are at low Galactic latitude and there is high extinction (NGC 6822, IC 0342, Maffei 1 and 2, for example) these same maps are useful, but the uncertainties are considerably larger. In these cases, spatial variations may not be resolved by the HI and IR maps that went into the tabulations, where “sub-grid” dust may be spatially quite patchy. Moreover, the conversion factors (gas-to-dust ratios, etc.) that go into converting HI and dust re-emission may also be variable across the sky, leading to imprecise predictions at any give position in the sky. Having a more direct means of determining the extinction to the TRGB stars themselves would, of course, be preferred.

To deal with these extreme cases of high extinction several novel approaches have been advanced by Tully and his collaborators: (1) For galaxies close to the Galactic plane the statistical color properties of the abundance of foreground red giant branch stars provide an estimation of line-of-sight reddening, as introduced and applied in Anand et al. (2019). (2) For highly-extincted galaxies, that also happen to have on-going star formation in their disks, then the redward displacement of the zero age main sequence can be used to estimate the total line-of-sight extinction. This provides an upper limit to the TRGB reddening given that the disk stars will also be suffering from *in situ* dust extinction that will not apply to the TRGB stars in the halo of that same galaxy.

Finally, for cases of intermediate extinction, such as the LMC, where comparable amounts of internal and foreground extinction are arising for a more centrally located (bar) population of TRGB stars, a differential, multi-wavelength comparison of observed tip magnitudes in the target galaxy (the LMC) with the corresponding tip magnitudes in a very low-reddening comparison galaxy (the SMC or IC 1613, for example) provide another path. In this application, high-precision tip detections, are required in at least three well-separated wavelength bands, resulting in the run of apparent distance moduli as a function of wavelength. These can then be fit by an adopted extinction curve, where the only remaining free parameter is the total line-of-sight extinction. This method is a generalization of a technique regularly used to de-redden extragalactic Cepheids (for a recent application, in that context, see Rich et al. 2018), and it has been successfully applied to the TRGB zero-point calibration recently published for the LMC by Freedman et al. (2020).

Ultimately, having a variety of estimates of the total line-of-sight reddening will, at very least, provide a better estimate of the systematic uncertainty to be associated with this correction. And, as it has been stated many times before, in many similar contexts, by moving as far into the infrared as possible, without sacrificing precision, will always reduce the impact of extinction, which continuously falls in its magnitude with increasing wavelength.

However, before proceeding further we provide visualizations of the coupled equations describing the interdependence of the slopes, zero points and mean magnitudes of the TRGB calibration across bands. Figures 1 & 2 show the calibrating equations for the near-infrared against a backdrop of  $JHK$  color-magnitude data for the galaxy IC 1613. The IC 1613 data are presented in Madore et al. (2018). Figure 3 is a simplified representation of the interconnected calibrations, going from the downward slanting  $V$ -band calibration, through the nearly-flat  $I$ -band TRGB, and then out into the near-infrared, where all of the calibrations trend upward with increasing color. This figure simultaneously illustrates the monotonic increase of the mean magnitude level of the TRGB population as a function of increasing wavelength. These multi-wavelength trends and correlations were all first illustrated in Figures 12 and 13 of Madore et al. (2018).

With multi-wavelength observations and their corresponding intrinsic calibrations of the TRGB, it is now possible to consider an alternative means of determining extinction corrections for the TRGB method using the tip stars themselves and for the same lines of sight being used for each galaxy individually. We now offer a first look at that possibility below.

### 3.1. *The Formulae for Determining Reddenings*

If we have three band passes ( $JHK$ , say) from which we can determine two independent *apparent* TRGB distance moduli, then it is possible to extract the reddening from the difference in these two moduli. However, because of the sloping nature of the color-magnitude description of the trace of the TRGB, the difference in apparent moduli is not simply the color excess. Using Figure 3 as a guide we can understand that the apparent distance modulus will be composed of *three terms*:  $\mu_o$ , the true distance modulus,  $A_\lambda$ , the extinction at the measured wavelength, and an additional term that numerically is the reddening multiplied by the slope  $a_\lambda$  of the intrinsic TRGB color-magnitude calibration. For instance

$$\mu_J = b_J - b_1 = \mu_J^o + A_J + a_1 E(J - H)$$

and

$$\mu_K = b_K - (b_1 - \beta) = \mu_K^o + A_K + (a_1 - \alpha)E(J - H)$$

Recognizing that  $\mu_J^o = \mu_K^o$ , this gives

$$\begin{aligned} \Delta\mu(JK) &= \mu_J - \mu_K = b_J - b_K + \beta \\ &= A_J + a_1E(J - H) - A_K - (a_1 - \alpha)E(J - H) \\ &= E(J - K) + \alpha E(J - H) \\ &= X_{JHK}E(J - H) + \alpha E(J - H) = (\alpha + X_{JHK})E(J - H) \end{aligned}$$

where

$$X_{JHK} = E(J - K)/E(J - H)$$

giving

$$E(J - H) = \Delta\mu(JK)/(\alpha + X_{JHK})$$

This means that, for the first time, it is in principle possible to determine directly and self-consistently the total line-of-sight extinction to the TRGB field using the TRGB stars themselves.

In the event that even more bandpasses are introduced, the value of the reddening will become over-constrained. At this point a scaled-extinction-curve fit to the apparent moduli as a function of wavelength will give a mean reddening and true modulus, as has been frequently done for determining these same parameters using multi-wavelength observations of extragalactic Cepheids (as first done by Freedman 1988; and more recently in Rich et al. 2014). Indeed, examples of an application of this approach using the near-infrared TRGB method can be seen in the simultaneous determination of the distance and reddening to the LMC, SMC and IC 1613 in Freedman et al. (2020).

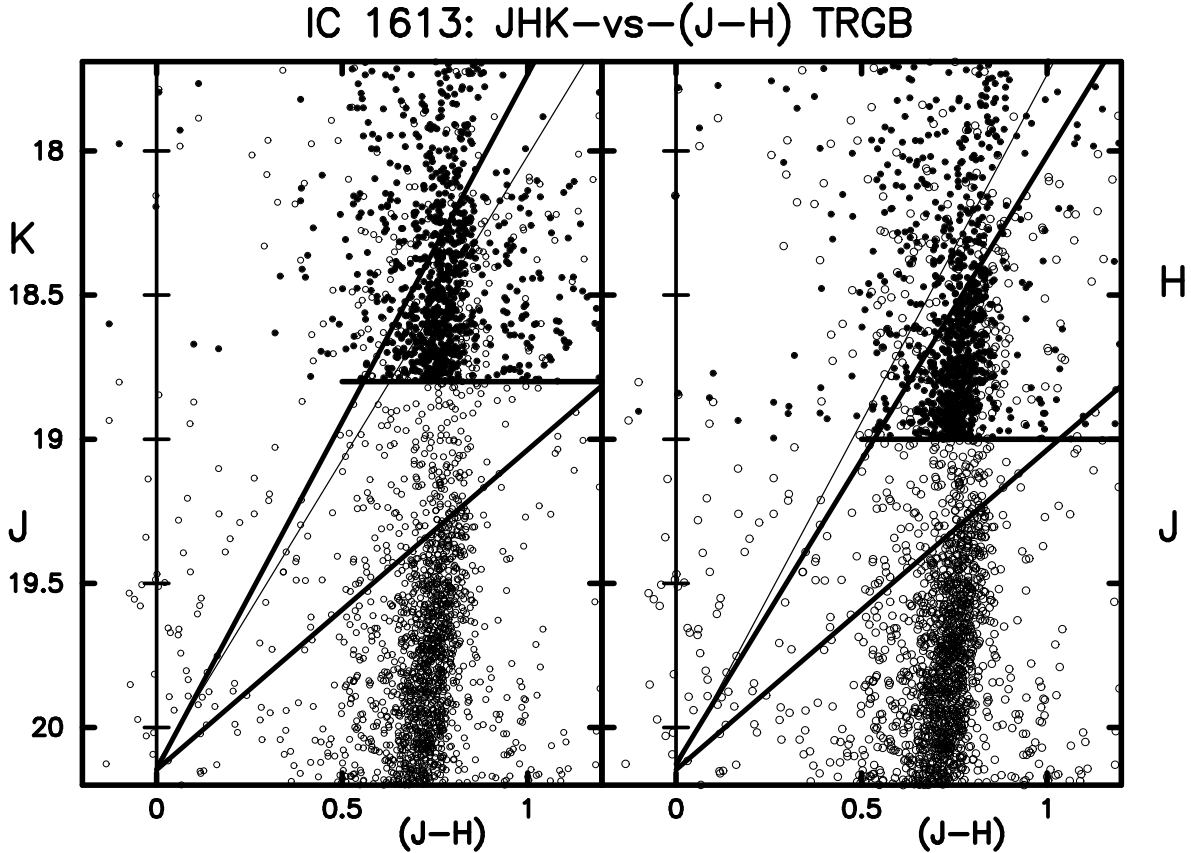


**Figure 1.** A montage of  $J, H, K$  vs  $(J - H)$  color-magnitude diagrams for IC 1613, centered on the upper magnitude of the TRGB and red giant branch. In the upper portion of the left plot is the  $K$ -band TRGB/CMD (small solid dots) truncated at  $K = 18.8$  mag. Upon this is superimposed the full  $J$ -band CMD (small open circles). The thick solid black lines mark the sloping TRGB, extrapolated to  $(J - H) = 0.00$  mag. The steeper line is a fit to the  $K$ -band data; the shallower line is a fit to the  $J$ -band TRGB. For clarity the  $H$ -band data and fits are presented in the right panel where the  $J$ -band data are reproduced. Thin solid lines give the fits to the data in alternate panels [i.e., the thin line in the left ( $K$ -band) panel is a muted rendering of the thick line ( $H$ -band) solution seen in the right panel, and vice versa] emphasizing how all three lines converge to the same Y intercept at  $(J-H) = 0.0$  mag

#### 4. SUMMARY AND CONCLUSIONS

We have explicitly provided the mathematical underpinnings of the color dependence of the magnitude of the TRGB as a function of wavelength and metallicity. In doing so we have emphasized the fact that for a given color the slopes and zero-point magnitudes are predetermined by the (distance-independent) intrinsic color-color relations between the various band passes being considered. It is a generic property of the TRGB calibration that at progressively longer wavelengths, the absolute magnitudes of the stars defining the TRGB will become brighter, in lock step with the slopes of



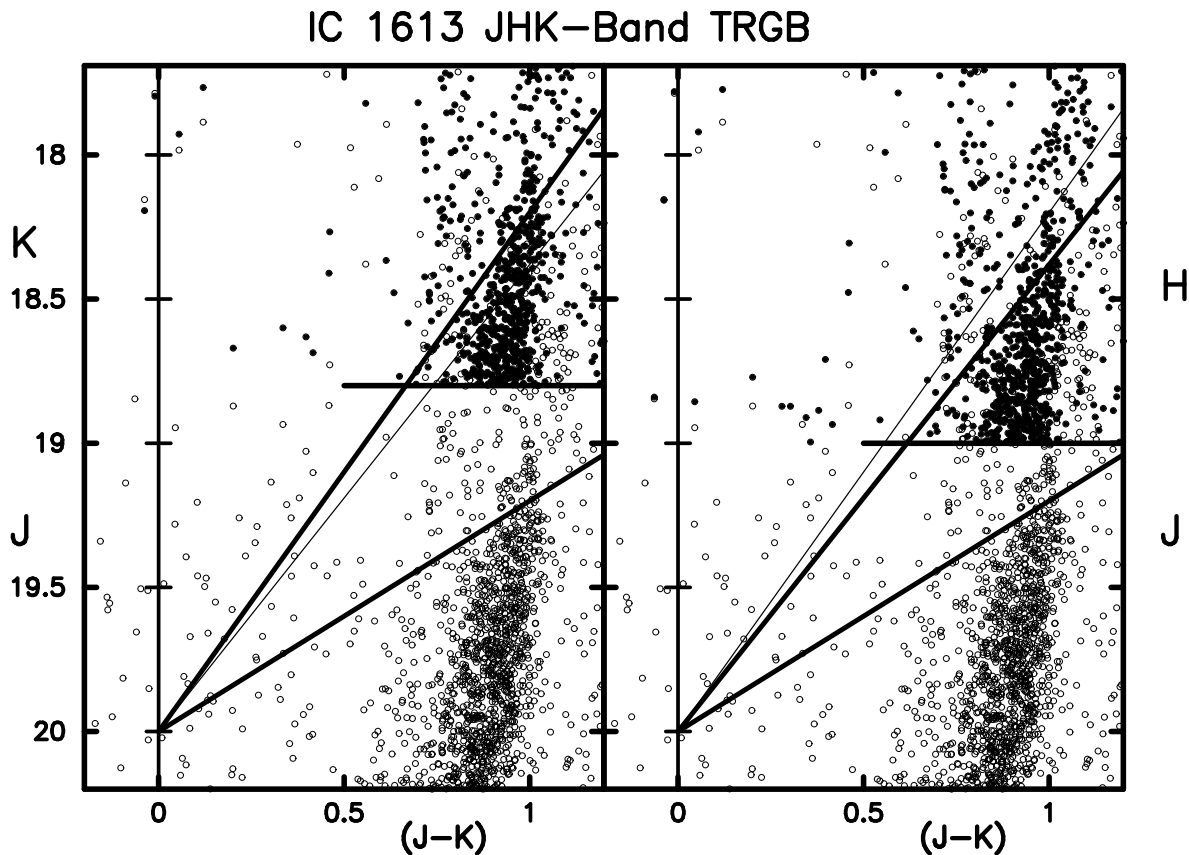


**Figure 2.** The same as Figure 1 in all respects except for a change in the color index. In this case the  $(J-K)$  color is being used.

the color-magnitude relation becoming steeper: longer wavelengths, steeper slopes, brighter absolute magnitudes. This simple property then provides a means to self-consistently correct TRGB magnitudes and distances for total line-of-sight reddening and extinction.

## 5. ACKNOWLEDGEMENTS

We thank the *Observatories of the Carnegie Institution for Science* and the *University of Chicago* for their support of our long-term research into the calibration and determination of the expansion rate of the Universe. The near-infrared observations discussed here were taken with the FourStar camera on the Baade 6.5m telescope at the Las Campanas Observatory, Chile. Support for this work was provided in part by NASA through grant number HST-GO-13691.003-A from the Space Telescope Science Institute, which is operated by AURA, Inc., under NASA contract NAS 5-26555. We thank Kayla Owens for her comments on a final draft of this paper; and finally, we thank the referee, Brent Tully, for his insightful perspectives on this method and its application.

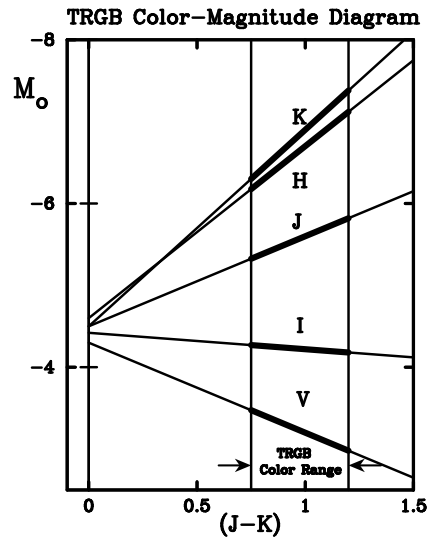


**Figure 3.** A purely graphical representation of the coordinated brightening of the absolute magnitude in step with the increasing slope of the TRGB with the increasing wavelength of the absolute magnitude being considered. The slopes and zero points are those of the calibrations presented in Madore et al. (2018) for the near-infrared calibration of the TRGB for IC 1613. See also Figure 1.

## 6. REFERENCES

- Anand, A.S., Tully, R.B., Rizzi, L. et al. 2019, *ApJ*, 880, 52  
 Beaton, R.L., Freedman, W.L., Madore, B.F. et al. 2016, *ApJ.*, 832, 210  
 Beaton, R.L., Seibert, M., Hatt, D. et al. 2019, *ApJ*, 885, 141  
 Birrer, S., Treu, T., Rusu, C.E. et al. 2018, *MNRAS*, 484, 4726  
 Bonvin, V., Courbin, F., Suyu, S.H. et al. 2017, *MNRAS*, 465, 4914  
 Burstein, D. & Heiles, C. 1982, *AJ*, 87, 1165  
 Dalcanton, J.J., Williams, B.F., Seth, A.C. et al. 2009, *ApJS*, 183, 67  
 Dalcanton, J.J., Williams, B.J., Melbourne, J.L. et al. 2012, *ApJS*, 198, 6  
 Demarque, P. & Geisler, J.E. 1963, *ApJ*, 137, 1102  
 Freedman, W.L. 1988, *ApJ*, 326, 691  
 Freedman, W.L., Madore, B.F., Gibson, B.K. et al. 2001, *ApJ*, 553, 47  
 Freedman, W.L., Madore, W.L., Scowcroft, V. et al. 2011, *AJ*, 142, 194  
 Freedman, W.L., Madore, B.F., Scowcroft, V. et al. 2012, *ApJ*, 758, 24  
 Freedman, W.L., Madore, B.F., Hatt, D., 2019, *ApJ*, 882, 34  
 Freedman, W.L., Madore, B.F., Hoyt, D., 2020, *ApJ*, 891, 57 arXiv: 2002.01550  
 Frogel, J., Cohen, J., & Persson, S.E. 1983, *ApJ*, 275, 773  
 Hartwick, F.D.A. 1968, *ApJ*, 154, 475  
 Hatt, D., Beaton, R.L., Freedman, W.L., et al. 2017, *ApJ*, 845, 146  
 Hatt, D., Freedman, W.L., Madore, B.F., et al. 2018a, *ApJ*, 861, 104

- Hatt, D., Freedman, W.L., Madore, B.F., et al. 2018b, ApJ, 866, 145
- Hoyt, T., Freedman, W.L., Madore, B.F. et al. 2018, ApJ, 858, 12
- Hoyt, T., Freedman, W.L., Madore, B.F. et al. 2019, pJ, 882, 150
- Jacobs, B.A., Rizzi, L., Tully, R.B., et al. 2009, AJ, 138, 322
- Jang, I.-S., Hatt, D., Beaton, R.L. et al. 2018, ApJ, 852, 60
- Jang, I.-S. & Lee, M.-G. 2017, ApJ, 836, 74
- Lee, M.-G., Freedman, W.L., & Madore, B.F. 1993, ApJ, 417, 553
- Madore, B.F., Freedman, W.L., Hatt, D. et al. 2018, ApJ, 858, 11
- McQuinn, K.B.W., Boyer, M., Skillman, E.D. et al. 2019, ApJ, 880, 63
- Planck Collaboration, Aghanim, N., Akrami, Y., et al. 2018, arXiv:1807.06209
- Rich, J., Persson, S.E., Freedman, W.L., Madore, B.F. et al. 2014, ApJ, 794, 107
- Rich, J.A., Madore, B.F., Monson, A.J. et al. 2018, ApJ, 869, 82
- Riess, A.G., Macri, L., Cassertano, S. et al. 2011, ApJ, 730, 119
- Riess, A.G., Macri, L., Hoffmann, S.L. et al. 2016, ApJ, 826, 56
- Riess, A.G., Cassertano, S., Yuan, W. et al. 2019, ApJ, 875, 145
- Salaris, M. & Cassisi, S. 1997, MNRAS, 289, 406,
- Sandage, A.R. & Wallerstein, G. 1960, ApJ, 131, 598
- Sandage, A.R. & Smith, L.L. 1966, ApJ, 144 , 886
- Schlafly, E.F. & Finkbeiner, D.P. 2011, ApJ, 737, 103
- Schlegel, D.J., Finkbeiner, D.P. & Davis, M. 1998, ApJ, 500, 525
- Scowcroft, V., Freedman, W.L., Madore, B.F. et al. 2016a, ApJ, 816, 49
- Scowcroft, V., Seibert, M., Freedman, W.L. et al. 2016b, MNRAS, 459, 1170
- Wu, P.-F., Tully, R.B., Rizzi, L., et al. 2014, AJ, 148, 7
- Wong, K. C., Suyu, S., H., Chen, G.C., et al. 2020, MNRAS, XXX, 1661, arXiv:1907.04869